IOP Publishing J. Phys. Mater. 5 (2022) 015002 https://doi.org/10.1088/2515-7639/ac3384

Journal of Physics: Materials

OPEN ACCESS

RECEIVED
6 July 2021

REVISED
1 October 2021

ACCEPTED FOR PUBLICATION
26 October 2021

PUBLISHED
23 November 2021

PAPER

Quasiparticle energies and optical response of $RbTiOPO_4$ and $KTiOAsO_4$

S Neufeld*, Arno Schindlmayr and W G Schmidt

Universität Paderborn, Department Physik, 33095 Paderborn, Germany
* Author to whom any correspondence should be addressed.

E-mail: sergejn@mail.upb.de

Keywords: DFT, rubidium titanyl phosphate, potassium titanyl arsenide, RTP, KTA, *GW* approximation, Bethe–Salpeter equation

Abstract

Many-body perturbation theory based on density-functional theory calculations is used to determine the quasiparticle band structures and the dielectric functions of the isomorphic ferroelectrics rubidium titanyl phosphate ($RbTiOPO_4$) and potassium titanyl arsenide ($KTiOAsO_4$). Self-energy corrections of more than 2 eV are found to widen the transport band gaps of both materials considerably to 5.3 and 5.2 eV, respectively. At the same time, both materials are characterized by strong exciton binding energies of 1.4 and 1.5 eV, respectively. The solution of the Bethe–Salpeter equation based on the quasiparticle energies results in onsets of the optical absorption within the range of the measured data.

1. Introduction

Polar ferroelectric oxides with the general constitution formula $MTiOXO_4$ are widely used in linear and nonlinear optics [1–5]. The most prominent members of this isomorphic crystal family (space group $Pna2_1$) are $KTiOPO_4$ (KTP), $RbTiOPO_4$ (RTP), and $KTiOAsO_4$ (KTA). They are characterized by TiO_6 octahedra and $(P, As)O_4$ tetrahedra that are linked by a common O atom, forming polyhedra chains along the [100] and [010] directions. The resulting cavities are occupied by eight- and ninefold coordinated alkali-metal atoms (K, Rb) that possess a high mobility along [001].

The fabrication of high-quality optical devices on the basis of KTP, KTA, and RTP, such as periodically poled waveguides for second-harmonic generation [2, 6–8], requires a thorough quantitative understanding of their electronic and optical properties. However, most theoretical studies addressing the band structure and dielectric function are restricted to the independent-particle level of theory [9–13], which causes a systematic underestimation of the excitation energies and thus a redshift of the optical absorption spectrum. In the case of KTP, self-energy effects are known to substantially widen the band gap compared to density-functional theory (DFT): in [14], an increase from 3.0 to 5.2 eV was reported. At the same time, strong exciton binding energies of the order of 1.5 eV were obtained. For RTP, there also exist indications for a strong influence of many-body effects on the electronic and optical excitation energies [15]. Experimentally, the valence-band density of states of KTA was measured with x-ray photoelectron spectroscopy [16]. From the data, in conjunction with full-potential linearized augmented-plane-wave calculations, the existence of two distinct O 2*s* sub bands was confirmed. The higher and lower energy band could be attributed to O atoms in a Ti–O–Ti and Ti–O–As bonding configuration, respectively. From investigations after Ar^+ ion bombardment of the pristine KTA sample, it was additionally concluded that the Ti–O–Ti bond strength exceeds that of the Ti–O–As bonds. Hansson *et al* [17], who measured polarized transmission spectra of KTP, RTP, and KTA, found that the (x, x) and (z, z) light polarization led to the largest and smallest transmission cutoff energies, respectively, for all three materials. Additionally, the transmission cutoff energies increased when going from KTA via RTP to KTP, with values ranging from 3.15 to 3.52 eV. Using absorption spectroscopy on KTP, Dudelzak *et al* [18] came to a similar conclusion: the Urbach parameter E_0, which corresponds approximately to the onset of the optical absorption, is largest for

the (x, x) and smallest for the (z, z) polarization. In spite of these measurements, a systematic study of trends in the electronic structure of the KTP family members is still missing, however.

This study aims at a deeper understanding of the electronic band structure and the optical response of RTP and KTA. In particular, we are interested in the similarities and differences of the optical excitation spectra of the KTP family materials, and we compare our calculated data with the available measurements. We employ many-body perturbation theory based on DFT. The calculations presented here are on the same footing as our recent study of KTP [14].

2. Computational method

The electronic ground state and the equilibrium geometries of RTP and KTA are determined from DFT using the Vienna Ab initio Simulation Package (VASP) [19]. Electronic exchange and correlation effects are described within the generalized gradient approximation using the PBEsol functional [20]. This functional is known to reproduce experimental lattice constants with high accuracy, typically with deviations from the measured data that are lower than 1% [21]. In the case of KTP, the deviation was shown in previous studies to be of the order of 0.5% [14, 22, 23]. The projector-augmented-wave technique [24] is used to describe the electron-ion interaction. In addition to all open shells, the O 2*s*, Ti 4*s*, Rb 4*p*, P 3*s*, K 3*p*, and As 4*s* orbitals are treated as valence states. The electronic wave functions are expanded into plane waves up to a cutoff energy of 500 eV. The Brillouin zone is sampled using a $2 \times 4 \times 2$ **k**-point mesh. In order to determine the ground-state geometries of RTP and KTA, a full structural relaxation is carried out until the force acting on each atom falls below a value of 0.01 eV Å^{-1}. The Kohn–Sham eigenvalues of both materials are calculated in **k** space along the path Γ–Y–T–Z–Γ (see [14] for notations). Based on the DFT band structure, the dielectric function is computed within the independent-particle approximation (IPA) as the weighted sum of single transitions between valence and conduction states [25, 26].

The quasiparticle energies are subsequently calculated within the non-self-consistent *GW* approximation for the electronic self-energy as implemented in VASP [27]. We use a cutoff energy of 300 eV, 1800 bands, and a $2 \times 4 \times 2$ **k**-point grid to determine the dynamically screened Coulomb interaction within the random-phase approximation. The dielectric function within the independent-quasiparticle approximation (IQA) is obtained in analogy to the IPA but includes the self-energy corrections to the DFT band structure. Given the large unit cells, the calculation of the quasiparticle shifts is computationally demanding. It requires more than three orders of magnitude more CPU time than needed for the self-consistent calculation of the electronic structure within DFT. On the other hand, the large unit cell together with the relatively small dispersion of the electron bands leads to a rapid convergence of the Brillouin-zone sampling. The quasiparticle energies obtained here are numerically converged within about 0.1 eV.

Finally, based on the quasiparticle energies, the Bethe–Salpeter equation (BSE) [28–30] is solved to include local-field and electron–hole interaction effects in the dielectric function. Again, a cutoff energy of 300 eV and a $2 \times 4 \times 2$ **k**-point mesh is used. The two-particle Hamiltonian is set up using 64 valence and 120 conduction bands. These parameters lead to a numerical convergence of the optical absorption energies better than 0.15 eV.

3. Results and discussion

The relaxed equilibrium lattice constants within PBEsol amount to $a = 12.986$ Å, $b = 6.521$ Å, $c = 10.568$ Å for RTP and $a = 13.181$ Å, $b = 6.607$ Å, $c = 10.791$ Å for KTA. Compared with the experimental values [5], we find a maximum deviation of about 0.5%, similar to KTP [14]. The different covalent radii of K/Rb and P/As have only a minor influence on the mean Ti–O bond lengths in RTP and KTA, amounting to 1.977 Å and 1.973 Å, respectively. For KTP a mean Ti–O bond length of 1.970 Å was reported [14]. These values are in excellent agreement with the measured bond lengths of 1.970 Å, 1.979 Å, and 1.966 Å for KTP, RTP, and KTA, respectively [31].

In figure 1, the electron band structures of RTP and KTA calculated on the DFT and *GW* levels of theory are shown. The direct DFT band gaps at Γ, 2.96 eV for RTP and 2.98 eV for KTA, are very close to the corresponding value of 2.97 eV for KTP [14]. The valence- and conduction-band edges consist predominantly of O 2*p* and Ti 3*d* states (see the density of states in figure 1). In addition, there is also a small contribution from As 4*p* states in the case of KTA. For both materials, self-energy corrections widen the band gap by more than 2 eV, leading to quasiparticle band gaps of 5.30 and 5.24 eV for RTP and KTA, respectively. This is very similar to KTP, where *GW* calculations widen the DFT band gap from 2.97 to 5.23 eV [14]. In KTA, the fundamental band gap is direct at the Γ point both in DFT and *GW*, whereas the valence-band maximum (VBM) of RTP shifts from Γ to T upon the inclusion of self-energy effects. As the conduction-band minimum (CBM) remains at Γ, the band gap thus becomes indirect. In the case of KTP,

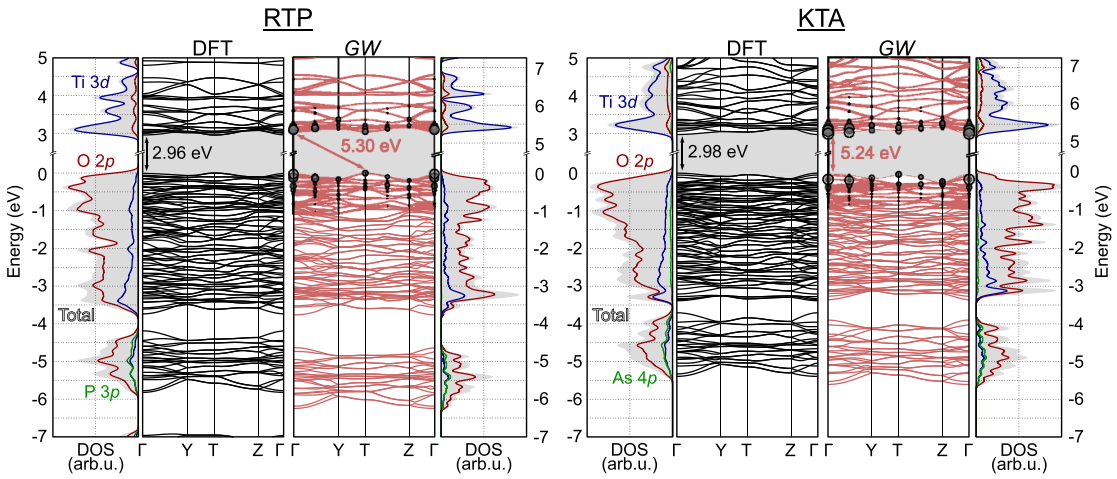

Figure 1. Comparison of the band structures and densities of states (DOS) of RTP (left) and KTA (right) calculated on the DFT and *GW* levels of theory. The relative contributions of transitions between valence and conduction bands to the first optical absorption peak are marked by circles in the *GW* band structure. The radii of the circles indicate the contribution of the electron–hole pair at that **k** point to the first exciton wave function.

the opposite was observed [14]: The VBM shifts from T to Γ upon the inclusion of quasiparticle effects, leading to a direct quasiparticle band gap. This suggests that the details of the band structure of the KTP family materials depend more sensitively on the species of the alkali-metal atoms than on the group-V atoms, at least close to the band edges. However, the effect is small, as the relative positions of the highest valence-band states at Γ and T differ by less than 20 meV. Moreover, these data should be interpreted with caution, given that the energy differences comparable to the numerical accuracy of the calculations. While the quasiparticle corrections widen the band gaps considerably, they affect the dispersion of the electron bands of all three KTP family materials only slightly.

Figure 2 shows the imaginary parts of the dielectric functions of RTP and KTA for the main polarization configurations (x, x), (y, y), and (z, z) calculated within the IPA, the IQA, and from the solution of the BSE. For comparison, we also show previous IPA and BSE results for KTP [14]. Generally, we find that the large quasiparticle shifts in the excitation energies are partially compensated by remarkably strong exciton binding energies in excess of 1 eV for all three materials. In particular, the dielectric functions of RTP and KTP are very similar, with a slightly higher absorption onset for RTP. As expected from the quasiparticle gaps, the onset of the dielectric function depends weakly on the occupation of the alkali sites, but even in the extreme case of a complete removal of all K (Rb) atoms from the KTA (RTP) matrix, the absorption onset is blueshifted by only 0.12–0.19 eV for all three polarizations within the IPA. On the BSE level, this blueshift reduces to 0.07–0.1 eV. The dielectric function of KTA differs notably from those of KTP and RTP for photon energies about 2 eV above the absorption onset: In this energy range, the optical absorption of KTA is clearly stronger than that of the other KTP family materials, especially for the (x, x) and (y, y) polarization. In order to explain this increase in the optical absorption, we analyze the dominant transitions in this energy region for the (x, x) component. Since qualitative trends in the optical absorption are typically reliably predicted on the IPA level, see, e.g. [26], we restrict our analysis to the IPA. We find that the enhanced absorption of KTA compared to RTP and KTP stems from transitions between pure O 2*p* valence states and empty states that involve both Ti 3*d* and hybrid O 2*p*/As 4*d* orbitals, as illustrated in figure 3. This hybrid character of the conduction states is only observed in KTA, whereas the corresponding states in KTP and RTP are of pure Ti 3*d* character; see the conduction-band state of KTP in [14] as an example. The group-V atom As or P thus affects the absorption characteristics for high-energy photons significantly.

Turning to the influence of many-body effects, we find that the inclusion of self-energy corrections in the IQA leads essentially to a rigid blueshift of the spectra by an amount equal to the *GW* quasiparticle shifts. The overall line shapes of the IQA and IPA spectra are very similar. Including excitonic effects in the dielectric functions by solving the BSE redshifts the calculated spectra. By evaluating the shift along the energy axis between the onsets of the optical absorption calculated within the BSE and IQA, we determine binding energies of 1.38 ± 0.12 eV and 1.51 ± 0.10 eV for the first bright excitons in RTP and KTA, respectively. This is similar to the exciton binding energy of 1.5 eV obtained for KTP [14], but larger than the prediction of 0.82 ± 0.17 eV by Ghoohestani *et al* [15] for RTP. The apparent discrepancy between this value and our results stems from the fact that Ghoohestani *et al* interpret the difference between the first main peak in the BSE spectrum and the minimum band gap of the quasiparticle band structure as the exciton binding

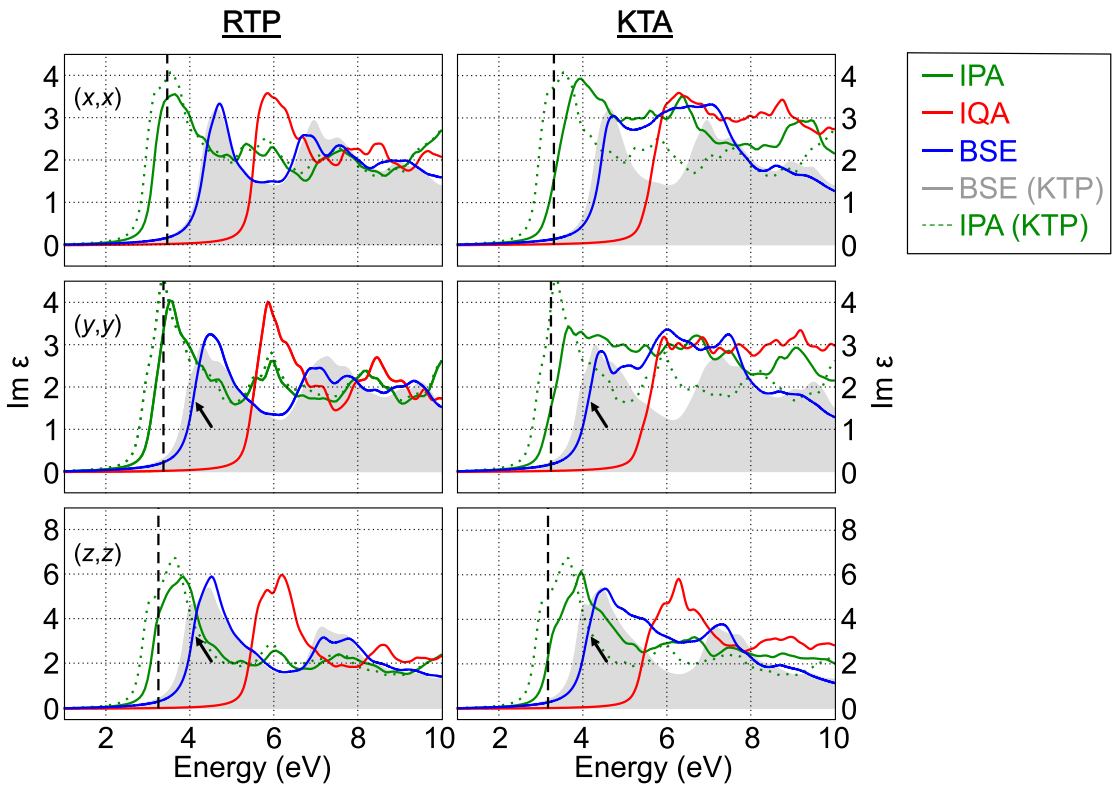

Figure 2. Dielectric functions of RTP (left) and KTA (right) calculated within the IPA, IQA, and BSE. For comparison, results for KTP are also shown. The first bright exciton corresponds to very weak shoulders in the BSE spectra marked by arrows. The vertical dashed lines indicate the positions of the experimentally determined absorption onsets [17].

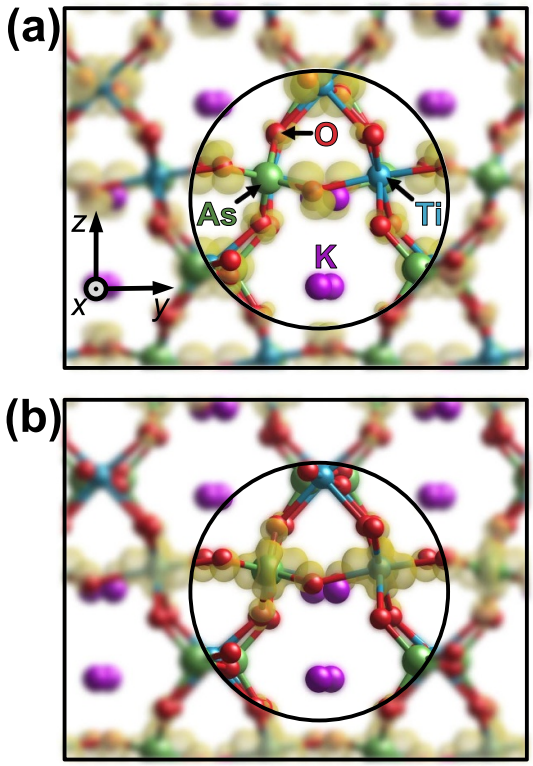

Figure 3. Charge densities of (a) the O 2*p* valence and (b) the Ti 3*d*—O 2*p*/As 4*p* conduction-band state of the transition that gives rise to the absorption peak at 6.3 eV within the IPA for the (x, x) polarization in KTA.

Table 1. Absorption onsets (in eV) of KTA and RTP calculated on the IPA, IQA, and BSE level of theory. For comparison, we also list our calculated values for KTP [14] as well as experimental data.

		Theory			Experiment		
Material		IPA	IQA	BSE	Reference [17]	Reference [18]	Reference [33]
KTA	(x,x)	2.98	5.33	4.15	3.29		
	(y,y)	2.90	5.27	3.80	3.22		
	(z,z)	2.83	5.17	3.74	3.15		
RTP	(x,x)	2.81	5.30	4.04	3.44		
	(y,y)	2.85	5.25	3.79	3.35		
	(z,z)	2.79	5.23	3.77	3.22		
KTP	(x,x)	2.79	5.27	3.99	3.52	4.30	2.95
	(y,y)	2.79	5.26	3.62	3.45	4.10	2.95
	(z,z)	2.70	5.09	3.59	3.39	3.98	2.95

energy. This leads to an underestimation, because the resonances in the BSE spectrum are not compared with their actual counterparts in the IQA, but rather with the energy of a direct transition between the VBM and the CBM, disregarding the oscillator strengths.

The dielectric functions of RTP and KTA are strongly anisotropic, and the strength of the first absorption peak varies for the different polarization directions. The first bright exciton corresponds to a very weak shoulder at about 4.1 eV in the BSE spectrum for both materials. Earlier results for RTP [15] already indicated that the excitonic wave function corresponds to a hole at oxygen, while the corresponding electron is localized at the Ti atoms. In order to relate these peaks to specific transitions in the band structures, we follow [32] and analyze the contributions of the electron–hole pairs to the first exciton wave function at the high-symmetry points of the Brillouin zone. The relative contributions are indicated by differently sized circles in the band structures of RTP and KTA in figure 1. Although all $\mathbf{k}$ points contribute, we find that the largest share stems from states close to Γ.

In agreement with experiment [17], see figure 2, we find the onset of the optical absorption to depend both on the material composition and on the polarization. The calculated onsets obtained by a linear extrapolation of the first absorption peaks on the energy axis for RTP, KTA, and KTP are listed in table 1. In agreement with the measured data [17], the optical absorption on the BSE level starts for the (z,z) polarization and is highest in energy for the (x,x) polarization, irrespective of the material. With the exception of the (z,z) polarization, we find that the cutoff energy decreases when going from KTA via RTP to KTP. This differs from the ordering KTP > RTP > KTA that is experimentally observed. However, a word of caution is in order. On the one hand, the energy differences calculated here are below the numerical accuracy of the present calculations. On the other hand, there are experimental uncertainties. First of all, the spectra may be affected by a poor sample quality as mentioned in [17]. The KTP family materials are prone to alkali-metal deficiencies [5]. As discussed above, this can be expected to modify the optical absorption onset. Indeed, Mangin *et al* [33] found a sharp increase of the optical absorption for all polarizations in flux-grown KTP already at 2.95 eV, i.e. at far lower energies than Hansson *et al* [17]. Secondly, the method to determine the absorption onset influences the result. While Hansson *et al* [17] used a cutoff criterion for the optical absorption of 2 cm^{-1}, Dudelzak *et al* [18] fitted the Urbach tail for various temperatures and thus deduced absorption onsets of 4.3, 4.1 and 3.98 eV for the (x,x), (y,y), and (z,z) polarization in KTP, respectively. These values are considerably larger than the data reported in [17, 33].

4. Conclusions

In this work, we report band-structure and optical-response calculations for the isomorphic ferroelectrics rubidium titanyl phosphate (RTP) and potassium titanyl arsenide (KTA). Our results show that the electronic transport band gaps in both materials are much larger than the optical band gaps measured in previous experiments [17]: we predict values of 5.30 and 5.24 eV for RTP and KTA, respectively. The details of the band edges seem to be more sensitive to an exchange of the alkali-metal ion than of the group-V atom. The optical absorption is affected by strong exciton binding energies of 1.38 ± 0.12 eV for RTP and 1.51 ± 0.10 eV for KTA. The first bright exciton in both materials is found to arise from transitions that involve essentially the complete Brillouin zone, with the largest contribution from its center. The stronger optical absorption of KTA compared to RTP for high-energy photons is related to transitions that involve empty As 4*p* orbitals. The optical absorption onset depends both on the material and on the polarization. It is predicted her to occur first for the (z,z) polarization in RTP and last for the (x,x) polarization in KTA.

Data availability statement

All data that support the findings of this study are included within the article (and any supplementary files).

Acknowledgments

Numerical calculations were performed using grants of computer time from the Paderborn Center for Parallel Computing (PC^2) and the HLRS Stuttgart. The Deutsche Forschungsgemeinschaft (DFG) is acknowledged for financial support (TRR 142—Project No. 231447078).

ORCID iDs

S Neufeld https://orcid.org/0000-0002-7693-098X
Arno Schindlmayr https://orcid.org/0000-0002-4855-071X

References

[1] Bierlein J D, Ferretti A, Brixner L H and Hsu W Y 1998 *Appl. Phys. Lett.* **50** 1216
[2] Cheng L K and Bierlein J D 1993 *Ferroelectrics* **142** 209
[3] Hagerman M E and Poeppelmeier K R 1995 *Chem. Mater.* **7** 602
[4] Rosenman G, Skliar A, Eger D, Oron M and Katz M 1998 *Appl. Phys. Lett.* **73** 3650
[5] Roth M 2010 Stoichiometry and domain structure of KTP-type nonlinear optical crystals *Springer Handbook of Crystal Growth* (Berlin: Springer) ch 20, pp 691–723
[6] Roelofs M G, Suna A, Bindloss W and Bierlein J D 1994 *J. Appl. Phys.* **76** 4999
[7] Risk W P and Loiacono G M 1998 *Appl. Phys. Lett.* **69** 4157
[8] Jiang Y *et al* 2006 *Appl. Phys. Lett.* **88** 011114
[9] Atuchin V V, Kesler V G, Meng G and Lin Z S 2012 *J. Phys.: Condens. Matter* **24** 405503
[10] Ghoohestani M, Arab A, Hashemifar S J and Sadeghi H 2018 *J. Appl. Phys.* **123** 015702
[11] Khyzhun O Y, Bekenev V L, Atuchin V V, Sinelnichenko A K and Isaenko L I 2009 *J. Alloys Compd.* **477** 768
[12] Lowther J E, Manyum P and Suebka S 2005 *Phys. Status Solidi* b **242** 1392
[13] Reshak A H, Kityk A V and Auluck S 2010 *J. Phys. Chem.* B **114** 16705
[14] Neufeld S, Bocchini A, Gerstmann U, Schindlmayr A and Schmidt W G 2019 *J. Phys. Mater.* **2** 045003
[15] Ghoohestani M, Hashemifar S J and Arab A 2020 *J. Appl. Phys.* **128** 125707
[16] Atuchin V, Khyzhun O Y, Bekenev V L, Sinelnichenko A K, Isaenko L I and Zhurkov S A 2013 *Proc. SPIE* **8772** 87721I
[17] Hansson G, Karlsson H, Wang S and Laurell F 2000 *Appl. Opt.* **39** 5058
[18] Dudelzak A, Proulx P P, Denks V, Mürk V and Nagirnyi V 2000 *J. Appl. Phys.* **87** 2110
[19] Kresse G and Furthmüller J 1996 *Phys. Rev.* B **54** 11169
[20] Perdew J P, Ruzsinszky A, Csonka G I, Vydrov O A, Scuseria G E, Constantin L A, Zhou X and Burke K 2008 *Phys. Rev. Lett.* **100** 136406
[21] Zhang G X, Reilly A M, Tkatchenko A and Scheffler M 2018 *New J. Phys.* **20** 063020
[22] Bocchini A, Eigner C, Silberhorn C, Schmidt W G and Gerstmann U 2020 *Phys. Rev. Mater.* **4** 124402
[23] Bocchini A, Neufeld S, Gerstmann U and Schmidt W G 2019 *J. Phys.: Condens. Matter* **31** 385401
[24] Kresse G and Joubert D 1999 *Phys. Rev.* B **59** 1758
[25] Del Sole R and Girlanda R 1993 *Phys. Rev.* B **48** 11789
[26] Schmidt W G 2005 *Phys. Status Solidi* b **242** 2751
[27] Shishkin M and Kresse G 2006 *Phys. Rev.* B **74** 035101
[28] Albrecht S, Reining L, Del Sole R and Onida G 1998 *Phys. Rev. Lett.* **80** 4510
[29] Rohlfing M and Louie S G 1998 *Phys. Rev. Lett.* **81** 2312
[30] Schmidt W G, Glutsch S, Hahn P H and Bechstedt F 2003 *Phys. Rev.* B **67** 085307
[31] Thomas P A, Mayo S C and Watts B E 1992 *Acta Crystallogr.* B **48** 401
[32] Bokdam M, Sander T, Stroppa A, Picozzi S, Sarma D D, Franchini C and Kresse G 2016 *Sci. Rep.* **6** 28618
[33] Mangin J, Khodjaoui A and Marnier G 1990 *Phys. Status Solidi* a **120** K111